Fluxgate Current Sensor Based on H-Bridge

Xinliang Tian
Hangzhi Precision Electronics Co. Ltd
Shenzhen, China

Qiyu Qian
Hangzhi Precision Electronics Co. Ltd
Shenzhen, China

Wei Fu
Hangzhi Precision Electronics Co. Ltd
Shenzhen, China

***Abstract*—In order to solve the technical problem that the detection accuracy of electric vehicle BMS current sensor is not high enough to accurately measure large current and small current at the same time, a design scheme of a fluxgate current sensor with a single excitation core was provided. The topology design and working principle of the scheme were expounded, and the advanced nature of the scheme was proved. Compared with the current scheme, the H-bridge circuit was used to drive the excitation coil, which enabled the power supply of a single power supply and simplified the design of the power supply for the sensor. Moreover, an excitation detection circuit with double measurement resistors was constructed, which equivalently converted the excitation current ie flowing in the excitation coil into the difference between the two currents i_{e1} and i_{e2}, and obtained the average value of the excitation current through the equivalent current difference i_{e1}-i_{e2}, thereby eliminating the zero drift of the current sensor, so that the small current identification and measurement accuracy of the current sensor can be improved.**

Keywords—Fluxgate, Current Sensor, H-Bridge, Differential equivalent current

I. INTRODUCTION

At present, the current monitoring of the battery management system (BMS) of electric vehicles mainly adopts the Hall current sensor [1-2]. Because it needs to disconnect the magnetic core and install the Hall chip, the sensitivity and resolution are reduced, the detection accuracy is not high enough, and the zero point drift and temperature drift are large, and it is difficult to meet the needs of high-precision current detection of electric vehicle battery packs [3-4]. The current sensor using fluxgate technology has the characteristics of high precision, small temperature drift and zero drift [5-9], and is suitable for BMS applications. However, the control power supply provided on the BMS of the electric vehicle is generally a single power supply, which requires a single power supply for the sensor power supply [10-12]. The traditional fluxgate current sensors are basically powered by positive and negative dual power supplies, and the positive and negative alternating square wave voltage of a certain frequency by the excitation oscillator is outputted to drive the excitation coil, so that the excitation coil generates an alternating excitation current, and the excitation core reaches the saturation state alternately [13-16]. In order to solve the above problems, this paper proposes a design method of fluxgate current sensor based on H-bridge.

II. H-BRIDGE TOPOLOGY DESIGN AND WORKING PRINCIPLE

The composition of the fluxgate current sensor based on H bridge and differential equivalent current is shown in Figure 1. The sensor includes a magnetic probe and an excitation detection circuit, which is used to measure the primary DC current I_d to be measured. The magnetic probe includes an excitation core and an excitation coil which is connected with the excitation detection circuit. The excitation core is an annular closed saturable soft magnetic core with high magnetic permeability, and the excitation core is used to carry the magnetic flux generated by primary DC current I_d to be measured and the magnetic field generated by the excitation current flowing in the excitation coil. The excitation coil is wound on the excitation core.

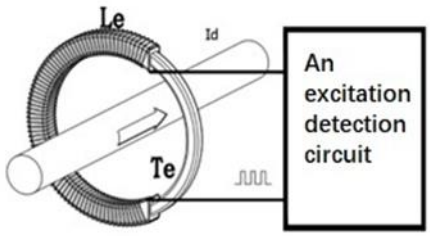

Fig. 1. The structure of the current sensor

The specific topology design of the sensor is shown in Figure 2. The magnetic probe of the sensor is composed of the excitation core T_e, the excitation coil L_e and the excitation coil impedance Re. The excitation coil is used to carry the alternating excitation voltage and excitation current constructed by the excitation detection circuit. The excitation detection circuit includes a DC voltage source Vdc, an H bridge circuit, and dual measurement resistors R_{e1} and R_{e2}. The DC voltage source Vdc provides power supply for the H-bridge circuit. The H-bridge circuit includes four switching device MOS tubes which have their own freewheeling diodes inside. The upper bridge arm of the H-bridge circuit is composed of PNP type MOS transistors Q_1 and Q_2, the lower bridge arm is composed of NPN type MOS transistors Q_3 and Q_4, the output end of the lower bridge arm Q_4 is connected to the positive end of the double measuring resistor R_{e1}, and the output end of lower bridge arm Q_3 is connected to the positive terminal of R_{e2}, and the negative terminals of R_{e1} and R_{e2} are both grounded.

The excitation detection circuit is used to output the alternating excitation voltage V_e to the excitation coil, which excites the excitation coil to generate the alternating excitation current i_e, and makes the excitation core reach the saturation state alternately. The construction method of the excitation voltage V_e is as follows: make the four switching devices in the H-bridge circuit turn on alternately, when the switching devices Q_1 and Q_4 are turned on, the switching devices Q_2 and Q_3 are turned off, and when the switching devices Q_1 and Q_4 are turned off, the switching devices Q_2 and Q_3 are turned on, so that an excitation voltage V_e with alternating positive and negative

Funded by Shenzhen Science and Technology Innovation [2021] No. 129

voltages at both ends of the excitation coil is constructed to excite the excitation coil.

The control method for controlling the alternating conduction of the four switching devices in the H-bridge circuit is as follows: by calculating the magnetic performance parameters and dimensions of the excitation core, the current threshold I_m that fully saturates the excitation core is obtained. In the design of the sensor, the current threshold I_m satisfies the following conditions, $I_m > | I_d / N_e |$, where I_d is the primary DC current value to be measured, and N_e is the number of turns of the excitation coil L_e. When the forward current value passing through the measurement resistor R_{e1} reaches the current threshold I_m, the switching devices Q_1 and Q_4 are turned off, and the switching devices Q_2 and Q_3 are turned on. When the forward current value passing through the measurement resistor R_{e2} reaches the current threshold value I_m, the switching devices Q_2 and Q_3 are turned off, and the switching devices Q_1 and Q_4 are turned on, so that the four switching devices in the H-bridge circuit are controlled to be turned on alternately by the peak value of the forward current flowing through R_{e1} and R_{e2}.

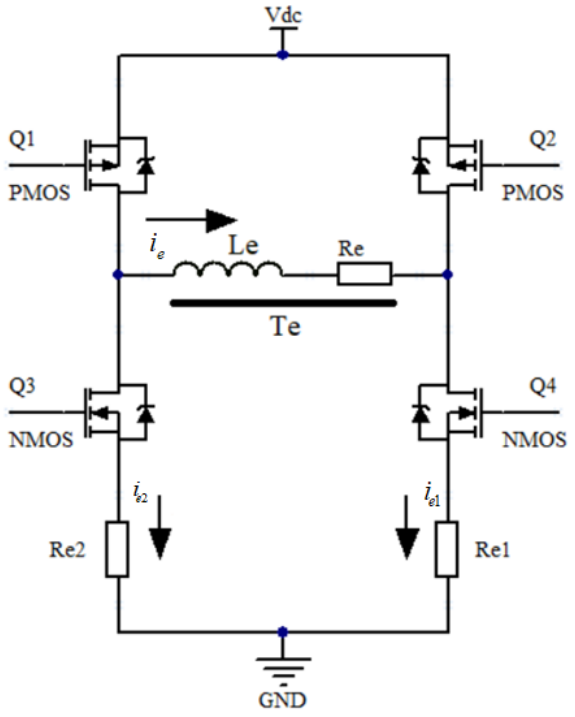

Fig. 2. H-bridge topology for current sensors

In addition, the excitation detection circuit is also configured to convert the excitation current i_e flowing in the excitation coil into the difference between the two currents i_{e1} and i_{e2} equivalently through the dual measurement resistors, where i_{e1} is the current flowing through the measurement resistor R_{e1}, i_{e2} is the current flowing through the measuring resistor R_{e2}, and then the average value of the excitation current flowing through the excitation coil is obtained through the difference equivalent current i_{e1}- i_{e2}, and then the value of the DC current I_d to be measured is obtained. The equivalent difference of currents i_{e1}- i_{e2} are designed to counteract the zero-point drift of the current sensor.

When the primary DC current I_d to be measured is zero, the magnetization curve of the current sensor excitation core T_e is shown in Figure 3. Under ideal conditions, the magnetization curve of the nonlinear excitation core T_e is in the form of a three-fold line [12]. where L and l represent the self-inductance of the excitation coil L_e when the excitation core T_e works in the linear region and the saturation region, respectively; ψ_s^+ and ψ_s^- represent the magnetic field when the excitation core T_e just reaches positive saturation and negative saturation, respectively chain; I_S^+ and I_S^- represent the positive and negative saturation currents of the exciting core T_e, respectively; I_m^+ and I_m^- represent the positive and negative maximum exciting currents of the exciting core T_e, respectively; V_H^+ and V_H^- represent the positive and negative peak values of the excitation voltage V_e, respectively. The excitation voltage V_e excites the nonlinear excitation core T_e to generate the excitation current i_e. Assuming that the circuit parameters are set reasonably, there are $I_m^+ = - I_m^- = I_m$, $I_S^+ = - I_S^- = I_S$ and $V_H^+ =- V_H^- = V_H$, and there is $I_m > I_S$, so as that the excitation magnet core T_e can be sufficiently saturated.

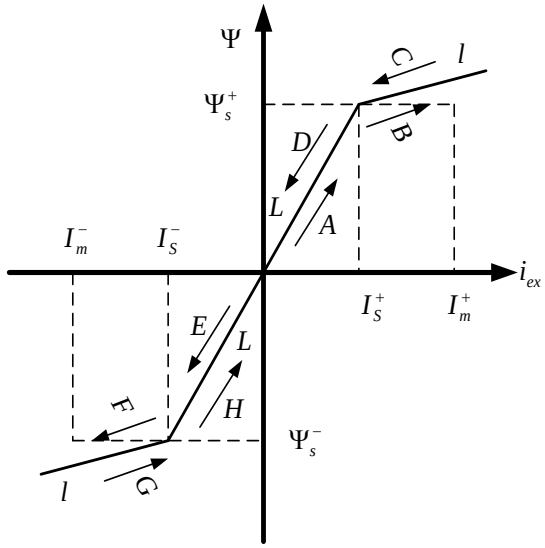

Fig. 3. The magnetization curve of the excitation core T_e

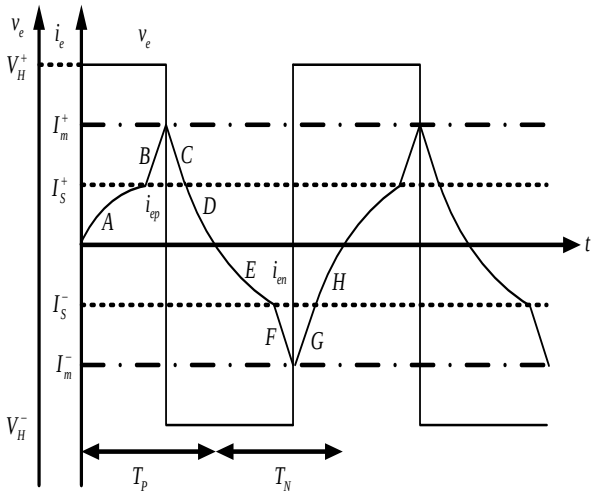

Fig. 4. Waveform diagram of excitation voltage and excitation current

When the primary DC current I_d to be measured is zero, the changes of the excitation voltage V_e and the excitation current i_e of the current sensor are shown in Figure 4. The working process of the H-bridge circuit is divided into the following four stages.

The first stage: Assuming that the MOS transistors in the switching devices Q_1 and Q_4 are turned on when the current sensor is powered on, the excitation core T_e works in the linear region A, the excitation voltage $V_e = V_H^+$ at both ends of the excitation coil, and the excitation current $i_e = 0$ in the excitation coil L_e, after power-on, the excitation current i_{ex} gradually increases from zero, and the excitation magnetic flux in the nonlinear excitation core T_e gradually increases. When the forward excitation current increases to $i_e = I_S^+$, the excitation core T_e reaches positive saturation. After that, the excitation core T_e enters from the linear region A to forward saturation region B, the self-inductance of the excitation winding W_1 changes from L to 1, the excitation impedance decreases, and the excitation current i_{ex} increases rapidly until $i_{ex} = I_m^+$.

The second stage: At this time, the switching devices Q_1 and Q_4 are turned off. Since the current in the exciting coil cannot be abruptly changed, the forward current of the switching devices Q_2 and Q_3 is freewheeling through the freewheeling diodes in the switching devices. This process can also be regarded as the connection of switching device Q_2 and Q_3 which have the same effect. At this time, the excitation voltage borne by both ends of the excitation coil $V_e = V_H^-$, the excitation core T_e goes from the forward saturation region B to the forward freewheeling regions C and D to work, and the forward excitation current i_e continues to decrease until $i_e = 0$, the diode forward freewheeling process ends.

The third stage: At this time, the MOS transistors in the switching devices Q_2 and Q_3 are turned on, the excitation voltage at both ends of the excitation coil $V_e = V_H^-$, and the excitation core T_e enters the negative linear region E and the negative saturation region F from the freewheeling region D, the negative excitation current i_e increases until $i_e = I_m^-$.

The fourth stage: At this time, the switching devices Q_2 and Q_3 are turned off. Since the current in the excitation coil cannot be abruptly changed, the negative current flows through the freewheeling diodes in the switching devices Q_1 and Q_4. This process can also be regarded as turning on the switching device Q_1 and Q_4, which have the same effect. At this time, the excitation voltage on both ends of the excitation coil $V_e = V_H^+$, the excitation core T_e goes from the negative saturation region F to the negative freewheeling regions G and H to work, and the negative excitation current i_e continues to decrease until $i_e = 0$.

At this time, the MOS transistors in the switching devices Q_1 and Q_4 are turned on, the excitation core T_e re-enters the linear region A to work, and the excitation core T_e repeatedly works from the A region to the F region according to the above working state, and repeats the above-mentioned first stage to fourth stage process.

The current sensor designed in this paper also includes an operational amplifier connected with the excitation detection circuit to adjust the gain and obtain the difference equivalent current i_{e1}-i_{e2}. At the same time, the ADC analog-to-digital converter which converts the analog signal into a digital signal, and the microprocessor MCU which calculates the average value of excitation current i_{av} and the DC current to be measured I_d are also included.

III. Method and Principle of Elimination of Zero Drift using Differential Equivalent Current

This scheme constructs an excitation detection circuit with double measuring resistors, and converts the excitation current i_e flowing in the excitation coil into the difference between the two currents i_{e1} and i_{e2}, and obtains the average value of the excitation current through the difference equivalent current i_{e1} - i_{e2}, to eliminate the zero drift of the current sensor. The zero point drift is caused by the inherent output zero point of the operational amplifier and ADC analog-to-digital converter every time the current sensor is powered on, and the inherent output zero point changes randomly within a certain range, which becomes the nonlinear error of the current sensor [18-19]. By comparing the influence of the zero point drift on the detection accuracy of the sensor when using the excitation current i_e and the difference equivalent current i_{e1} - i_{e2} to obtain the excitation average current, it is proved that by constructing the difference equivalent current i_{e1} - i_{e2} to eliminate the current sensor zero drift is effective.

A. Obtained by the Excitation Current i_e

When the DC current I_d to be tested is zero, the waveform of the excitation current i_{e1} of the excitation coil is shown in Figure 4. A working cycle T of the excitation current is divided into a positive half cycle TP and a negative half cycle TN. The excitation current i_e is positive i_{ep} during the positive half cycle TP, and the excitation current i_e is the negative current i_{en} during the negative half cycle TN, with $i_e = i_{ep} + i_{en}$. Ideally, the positive and negative half-cycle waveforms of the excitation current i_e are symmetrical, so the average value i_{ay} of the excitation current i_e in one cycle is equal to zero.

However, the operational amplifier and ADC analog-to-digital converter used in the signal gain adjustment and sampling process will output a changing inherent zero every time the power is turned on or the external environment changes. The zero point drift generated by the output zero point is converted into the excitation current of the excitation coil equal to the constant ΔI_e, and the constant ΔI_e can be understood as a constant ΔI_e superimposed on the sampling value of each excitation current Ie than the actual value, which is equivalent to a constant ΔI_e, the same amount of the curve of the excitation current ie in Figure 4 shifted upwards.

Therefore, the zero drift will cause the actual value of the primary DC current Id to be measured to be 0, the average value of the excitation current i_{av} is not equal to 0, $i_{av} = \Delta I_e$, and then the calculated value I_{dd} of the primary DC current I_d to be measured is not equal to 0, Therefore, the current sensor produces a zero point drift error, and the error will be different every time it is powered on, and it is randomly distributed within a certain error range, so it cannot be calibrated.

Assuming that the rated range of the current sensor is 500A, according to experience, the error caused by the above zero drift is about one ten-thousandth of the rated range of the current sensor, that is, 50mA. Therefore, when the current sensor adopts the method of obtaining the average excitation current through

the excitation current ie, the current sensor will not be able to measure the small current less than 50mA, thus affecting the small current recognition and measurement accuracy of the current sensor.

B. Obtained by the Differential Equivalent Current i_{e1}-i_{e2}

The four switching devices in the H bridge circuit of the present invention are turned on alternately in pairs, and one switching device on the upper bridge arm of the H bridge must be turned on at the same time as one switching device on the lower bridge arm of the H bridge, so the two switching devices of the upper bridge arm of the H bridge or the two switching devices of the lower bridge arm of the H bridge will never be turned on at the same time, the excitation current i_e flowing through the excitation coil must flow through the double measuring resistors R_{e1} and R_{e2} to form a current loop, and the exciting current ie always flows only through the only measuring resistor R_{e1} or R_{e2}. When the switching devices Q1 and Q4 are turned on, the exciting current i_e flows through the resistor R_{e1}. At this time, it is defined that the exciting current ie is in the same direction as the current on the resistor R_{e1}; when the switching devices Q2 and Q3 are turned on, the exciting current i_e flows through the resistor R_{e2}, and the current direction of excitation current ie and the resistor R_{e2} are opposite. So the excitation current ie is equal to the difference equivalent current i_{e1}-i_{e2}, that is, $i_e=i_{e1}$-i_{e2}, the excitation current i_e flowing in the excitation coil is equivalently converted into the difference between the two currents of i_{e1} and i_{e2} through the double measuring resistors R_{e1} and R_{e2}.

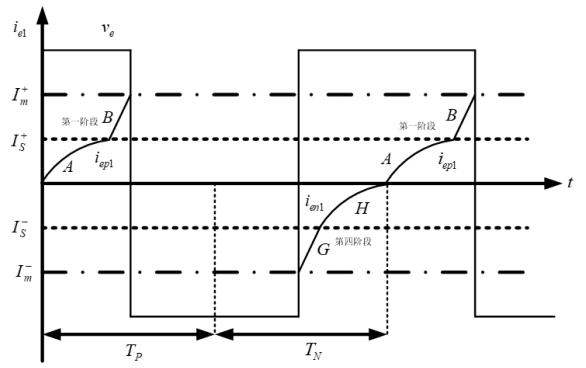

Fig. 5. The waveform of the current flowing through the measurement resistor R_{e1} in one cycle

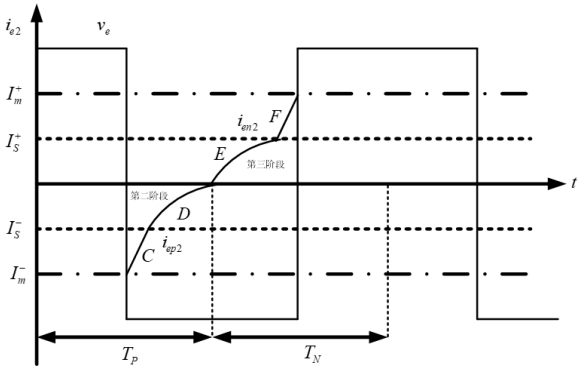

Fig. 6. The waveform of the current flowing through the measurement resistor R_{e2} in one cycle

As shown in Figure 5 and Figure 6, they are the current waveforms flowing through the measured resistors R_{e1} and R_{e2} in one cycle respectively. Compared with the excitation current waveform shown in Figure 4, it can be seen that the forward excitation current i_{ep} is converted into a positive current i_{ep1} on R_{e1} and negative current i_{ep2} on R_{e2} through measuring resistor. The negative excitation current i_{en} is converted into the positive current i_{en2} on R_{e2} and the negative current ien1 on R_{e1} through measuring resistor. So the following equation is established:

$$i_{ep}=i_{ep1}-i_{ep2} \tag{1}$$

$$i_{en}=i_{en1}-i_{en2} \tag{2}$$

$$i_e=i_{ep}+i_{en}=i_{ep1}+i_{en1}-i_{ep2}-i_{en2}=（i_{ep1}+i_{en1}）-（i_{ep2}+i_{en2}）=i_{e1}-i_{e2} \tag{3}$$

i_{ep1} and i_{en1} are the currents flowing on the measuring resistor R_{e1}, and i_{ep2} and i_{en2} are the currents flowing on the measuring resistor R_{e2}. Based on the equation (3), the exciting current i_e of the excitation coil is equal to the current difference i_{e1}-i_{e2} flowing through the dual measuring resistors R_{e1} and R_{e2}.

It can be seen from the above description that this scheme converts the positive excitation current i_{ep} into positive current flow i_{ep1} and negative current i_{ep2}, and converts negative excitation current i_{en} into positive current i_{en2} and negative current i_{en1} through double measuring resistances R_{e1} and R_{e2}. This constitutes a necessary condition for the subsequent calculation of the excitation average current through the difference equivalent current.

When the primary DC current I_d to be measured is zero, it is assumed that the zero point drift generated by the inherent output zero point of the operational amplifier and ADC analog-to-digital converter is converted into the excitation current of the excitation coil with the amount of constant ΔI_e, which means that the current curves of the currents i_{e1} and i_{e2} across the double measuring resistors R_{e1} and R_{e2} are shifted upwards by a constant ΔI_e in Figure 5 and Figure 6.

However, since the positive excitation current i_{ep} is converted into positive current i_{ep1} and negative current i_{ep2}, it is assumed that the number of sampling points for positive current i_{ep1} and negative current i_{ep2} are constant N in the process of obtaining the average current i_{avp} of positive excitation for one cycle, the sampling value of the positive current i_{ep1} is i_{ep11} to i_{ep1N}, and the sampling value of the negative current i_{ep2} is i_{ep21} to i_{ep2N}, then there is the following formula (4):

$$i_{avp}=\frac{[(i_{ep11}+\Delta I_e)+(i_{ep12}+\Delta I_e)+\cdots\ldots(i_{ep1N}+\Delta I_e)]-[(i_{ep21}+\Delta I_e)+(i_{ep22}+\Delta I_e)+\cdots\ldots(i_{ep2N}+\Delta I_e)]}{2N}$$

$$=\frac{(i_{ep11}+i_{ep12}+i_{ep1N})-(i_{ep21}+i_{ep22}+i_{ep2N})}{2N} \tag{4}$$

It can be known from equation (4) that in the process of obtaining the average positive excitation current i_{avp} of one cycle, since the constant ΔI_e in the positive current i_{ep1} and the negative current i_{ep2} cancel each other out in the process of obtaining the difference, excitation current error ΔI_e from the zero point drifts does not affect the calculation of the positive excitation average current i_{avp}, and does not bring zero drift error.

Similarly, the negative excitation current i_{en} is converted into positive current i_{en2} and negative current i_{en1}, assuming that the number of sampling points for positive current i_{en2} and negative current i_{en1} are constant N in the process of obtaining the average current i_{avn} of negative excitation for one cycle, the sampling value of the negative current i_{en1} is i_{en11} to i_{en1N}, and the sampling value of the positive current i_{en2} is ien21 to i_{en2N}, then there is the following formula (5):

$$i_{avn} = \frac{[(i_{en11}+\triangle I_e)+(i_{en12}+\triangle I_e)+\cdots(i_{en1N}+\triangle I_e)]-[(i_{en21}+\triangle I_e)+(i_{en22}+\triangle I_e)+\cdots(i_{en2N}+\triangle I_e)]}{2N}$$

$$= \frac{(i_{en11}+i_{en12}+i_{en1N})-(i_{en21}+i_{en22}+i_{en2N})}{2N} \quad (5)$$

It can be known from equation (5) that in the process of obtaining the average negative excitation current i_{avn} of a cycle, since the constant ΔI_e in the positive current ien2 and the negative current ien1 cancel each other out in the process of obtaining the difference, excitation current error ΔI_e from the zero point drifts does not affect the calculation of the negative excitation average current i_{avp}, and does not bring zero drift error..

Equation (4) and equation (5) obtain the positive excitation average current i_{avp} and the negative excitation average current i_{avn} of one cycle, and the excitation average current i_{av} of one cycle can be obtained, $i_{av}=i_{avp}+i_{avn}$.

Further, according to the excitation average current i_{av}, the calculated value I_{dd} of the primary DC current Id to be measured can be obtained, $I_{dd}=i_{av}\times N_e$, where N_e is the number of turns of the excitation coil L_e.

When the primary DC current Id to be measured is zero, in an ideal state, the positive excitation average current i_{avp} and the negative excitation average current i_{avn} are equal but opposite in direction, so the average value i_{av} of the excitation current i_e in one cycle is equal to zero, and then the calculated value I_{dd} of the primary DC current I_d to be measured is also equal to 0.

From the above derivation, it can be known that calculating the average excitation current through the difference equivalent current i_{e1}-i_{e2} can eliminate the error caused by the zero point drift, and then eliminate the error caused by the zero point drift to the primary DC current to be measured of the current sensor.

If the rated range of the current sensor is set to be 500A, according to the actual results, after using the method of obtaining the average excitation current by using the difference equivalent current i_{e1}-i_{e2}, the current sensor developed by the present invention can measure a small current of 5mA, the recognition degree of the sensor is 2mA. Compared with the method of obtaining the average excitation current directly through the excitation current ie, the small current recognition degree and measurement accuracy of the current sensor are improved. In addition, this technical solution can be applied to the leakage current sensor to detect milliampere-level microcurrent [20]. The leakage current sensor developed in this scheme can measure the microcurrent of 1mA, and the recognition degree of the current sensor is 0.1 mA.

IV. Product Development and Test Results

The accuracy error test results of the 300A current sensor developed according to the technical solution in this paper are shown in Figure 7. The measurement current range is -330A≤ I_d≤+330A, and the test temperature range is -40° to 85° . The measurement error is expressed in absolute error mA, and the maximum allowable error is the relative error expressed as a percentage, which is 0.5%. The test results show that the full temperature and full scale range of the sensor can meet the requirements, and the error is basically within 0.2%.

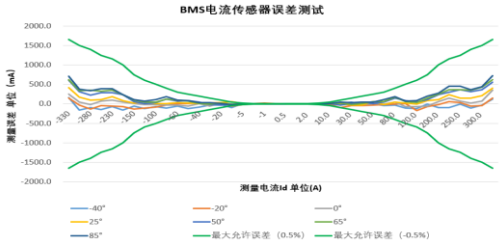

Fig. 7. Error test result graph of current sensor

According to the above technical solutions in this article, the 300A and 500A automotive BMS current sensor products developed by Shenzhen Hangzhi Precision Electronics Co., Ltd. are shown in Figure 8. They have independent intellectual property rights, low temperature drift, low zero drift, high temperature resistance, and advanced technical performance indicators.

Fig. 8. Sensor product display

The technical parameters of the current sensor shown in the above figure are shown in Table I below.

TABLE I. Technical Parameters

Measuring range	±300A/ ±500A
Power	7 – 18V
Aperture	24.2mm
Output	CAN
Working temperature	-40 - 85℃
Accuracy	< 0.5%
Linearity	< 0.1%
The adapter connector	TE MPN 1473672-1
High reliability	Multiple self-check, multiple hardware protection, CRC check to ensure reliable communication

V. Conclusion

In this paper, a design method of a fluxgate current sensor based on H-bridge is proposed, the topology design and working principle of the scheme are expounded, and the advanced nature of the scheme is proved, and an automotive BMS current sensor with advanced performance is manufactured according to the

scheme. In the sensor, the H-bridge circuit is used to drive the excitation coil. By controlling the conduction of different bridge arms of the H-bridge, the positive and negative alternating excitation voltage can be output at both ends of the excitation coil by using a single power supply. Compared with the excitation circuit of the traditional positive and negative power supply, it simplifies the design of the sensor power supply. The product can be widely used in the field of automotive BMS current sensor and DC leakage current detection.

REFERENCES

[1] Zhang H Z, Li Y S, Liu J, Design of magnetic ring for split Hall current sensor for calibration [J]. Electrical Measurement & Instrumentation, 2022, 59(02) : 171-175

[2] Xie Z Y, Zhang C, Xie S Z, Design of Optimal Algorithm for Deeccentricity Error of Arrayed Hall Sensor [J]. Electrical Measurement & Instrumentation, 2022, 57(22) : 133-138

[3] TIAN X L, QIAN Q Y, FU W, Multi-point zero flux technology of the fluxgate current transducers [J], Electrical Measurement & Instrumentation, 2018, 55(S1): 21-25.

[4] TIAN X L, QIAN Q Y, FU W, Fluxgate Current Transducer based on Multi-point Zero Flux Technology[C], Proceedings of 2018 International Conference on Power System Technology (POWERCON 2018), 2018: 1056-1061.

[5] E. G. Coker, H Can, S Selvi, Design of a DC current sensor based on fluxgate principle, Proceedings of Applied Physics of Condensed Matter (APCOM 2019), July 2019 [C]:020007, 1-3.

[6] ZHANG X F, LU Y L, Fluxgate Technology [M], Beijing, National Defense Industry Press, 1995.

[7] Cui Z J, Closed-loop feedback broadband fluxgate design [J]. Instrument technology and sensors, 2018(3): 117-121

[8] WANG L W, WANG X, FENG Z K, Design and verification of magnetic modulation sensor based on half-wave excitation［J］. Journal of Sensing Technology, 2015, 28(10) : 1448-1453.

[9] Yan Q, Li X S, Ye Y Y, et al, Research on High Precision Phase Difference Magnetic Modulation DC Sensor［J］. Electrical Measurement & Instrumentation, 2021, 58(12): 144-148.

[10] L. Schrittwieser, M. Mauerer, D. Bortis, G. Ortiz, J. W. Kolar, Novel principle for flux sensing in the application of a DC + AC current sensor[J]. IEEE Transactions on Industry Applications, 2015, 51(5): 4100-4110.

[11] Xiaoguang Yang, Wei Guo, Congcong Li, Bo Zhu, Tanggong Chen, Wenqi Ge, Design optimization of a fluxgate current sensor with low interference[J]. IEEE Transactions on Applied Superconductivity, 2016, 26(4): 1-5.

[12] CAO M, Research on key technology and test system construction of battery management system, Doctoral Dissertation of Nanchang University, 2020, 12.

[13] O Mironenko, W Kempton, Comparing Devices for Concurrent Measurement of AC Current and DC Injection during Electric Vehicle Charging[J], World Electric Vehicle Journal, 2020, 11(3), 57

[14] X. Yang, Xiaoguang Yang, Wei Guo, Congcong Li, Bo Zhu, A fluxgate current sensor with a U-Shaped magnetic gathering shell[J]. IEEE Transactions on Magnetics, 2015, 51(11): 1-4.

[15] Cheng Jian, Hao Yaodou, Zhang Jing, Development of a zero flux error transductor for the DC power supply with high current stability[J], Atomic Energy Science and Technology, 2002, 36(3): 250-252

[16] Zhang Peng, Feng Zhuoming, Song Qinghua, Wu Yongquan, Wu Jianping, Study on Parameter Optimization Method of Self‐oscillating Fluxgate Current Sensor[J], Instrument Technique and Sensor, 2021, (12): 34-37

[17] WANG N, Self-oscillating fluxgate technology for precision measurement of DC high current, Doctoral Dissertation of Harbin Institute of Technology, 2016, 6.

[18] ZHU Y K, WANG Y Q, Application of sensor technology in BMS and countermeasures[J], Automobile Maintenance, 2022, 3(01): 18-21.

[19] LEM. Isolated Current and voltage transducers, 3rd Edition[M]. LEM Corporation. 2004.

[20] WU Y, LI K, WANG Y, et al. Analysis and simulation of dynamic process of excitation current of magnetic modulation residual current transformer[J], Transactions of China Electrotechnical Society, 2014, 29(7): 244-252.